Research Article

For reprint orders, please contact: reprints@futuremedicine.com

Nanomedicine

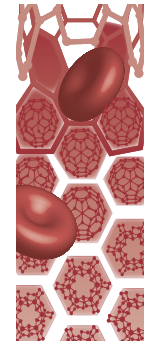

Development and characterization of a long-acting nanoformulated abacavir prodrug

Aim: A myristoylated abacavir (ABC) prodrug was synthesized to extend drug half-life and bioavailability. **Methods**: Myristoylated ABC (MABC) was made by esterifying myristic acid to the drug's 5-hydroxy-cyclopentene group. Chemical composition, antiretroviral activity, cell uptake and retention and cellular trafficking of free MABC and poloxamer nanoformulations of MABC were assessed by proton nuclear magnetic resonance and tested in human monocyte-derived macrophages. Pharmacokinetics of ABC and nanoformulated MABC were evaluated after intramuscular injection into mice. **Results:** MABC antiretroviral activity in monocyte-derived macrophages was comparable to native drug. Encasement of MABC into poloxamer nanoparticles extended drug bioavailability for 2 weeks. **Conclusion:** MABC synthesis and encasement in polymeric nanoformulations improved intracellular drug accumulation and demonstrate translational potential as part of a long-acting antiretroviral regimen.

First submitted: 15 April 2016; Accepted for publication: 14 June 2016; Published online: 26 July 2016

Keywords: abacavir prodrug • antiretroviral therapy • monocyte-macrophages • nanoformulated antiretrovirals • pharmacokinetics

Dhirender Singh[1,2], JoEllyn McMillan[2], James Hilaire[2], Nagsen Gautam[1], Diana Palandri[2], Yazen Alnouti[1], Howard E Gendelman*[,1,2] & Benson Edagwa[2]

[1]Department of Pharmaceutical Sciences, University of Nebraska Medical Center, Omaha, NE, USA

[2]Department of Pharmacology & Experimental Neuroscience, University of Nebraska Medical Center, Omaha, NE, USA

*Author for correspondence:
Tel.: +1 402 559 8920
Fax: +1 402 559 3744
hegendel@unmc.edu

Treatment of HIV infection mandates early and lifelong treatment with combination antiretroviral therapy (cART) [1]. One impediment in reaching successful clinical outcomes is lack of adherence to cART drug regimens that serve to sustain reductions in viral load and maintain $CD4^+$ T lymphocyte numbers [2,3]. Maintaining cART drug levels is essential to protect susceptible cell populations and enable sustained antiviral responses to preclude the development of viral resistance [1]. Lack of achievement of effective treatment outcomes rests in the inabilities of drugs to specifically target viral reservoirs [4]. These include gut-associated lymphoid tissue, lymph nodes, spleen, the CNS and specifically central memory lymphocytes and myeloid cells contained within the lymphoreticular tissues [5–7]. Limitations in drug bioavailability have affected therapeutic outcomes [8]. All can lead to the perpetuation of viral sanctuaries and accelerate cART failures [9,10]. We posit that the development of long-acting viral reservoir-targeted nanoformulated ART (nanoART) can overcome such limitations while reducing drug toxicity and metabolism, improving drug targeting and facilitating slow release of cell-carried drug cargos. These ultimately serve to improve antiretroviral drug pharmacokinetics (PK) and pharmacodynamics [11–15]. To such ends, our laboratory has pioneered the development of nanoART [16–19]. Our nanoformulations show further improvements in design through ligand surface engineering [13,19] serving to facilitate uptake into virus target cells. Mononuclear phagocytes (MPs; monocytes, macrophages and dendritic cells) serve as drug carriers. These cells facilitate drug carriage through their mobility, rapid delivery, cargo encasements and abilities to deploy

Future Medicine part of fsg

drug to viral target tissues [20]. To such ends, the ability of nanoART to home drug depots to viral reservoirs represents notable advantages over conventional therapy [21]. This explains the need for an interdisciplinary program serving to encapsulate antiretroviral drugs into polymeric nanoparticles for MP drug delivery and enabling PK and pharmacodynamics testing [16,17,19,22].

An obstacle toward success has been the difficulty in formulating the many available hydrophilic antiretroviral drugs into nanoparticles for parenteral administration. Thus, a platform was constructed to convert the drug abacavir (ABC) into a hydrophobic compound through esterification using myristic acid. Of interest, fatty acid analogs of myristic acid can inhibit *N*-myristoyltransferase, an enzyme that catalyzes myristoylation, which is needed for activity of several proteins involved in the life cycle of HIV [23–27]. With this in mind, myristoylated ABC (called MABC) was synthesized and then formulated into nanosuspensions. This enabled the formation of hydrophobic drug crystals that were then placed into poloxamer-coated nanoparticles. Improved antiretroviral activity was observed for the modified ABC. Prolonged antiretroviral activity was realized with the establishment of drug depots in Rab endosomes. Prolonged drug MP carriage and PK support the opinion that MABC holds promise to extend the drug armamentarium for HIV/AIDS therapy.

Materials & methods

Chemicals

ABC sulfate, myristic acid, poloxamer 407 (P407), folic acid (FA) and CF633-succinimidyl ester were purchased from Sigma-Aldrich (MO, USA). ABC sulfate was converted into free-base using sodium bicarbonate. The chemical reactions were performed under a dry argon atmosphere. Flash chromatography was performed using 32–63-µm flash silica gels from Dynamic Adsorbents, Inc. (GA, USA). Reactions were followed by thin-layer chromatography on precoated silica plates (250 µm) F-254 from SiliCycle, Inc. (QC, Canada). The compounds were visualized by ultraviolet fluorescence or by staining with ninhydrin or $KMnO_4$ stains. HPLC-grade methylene chloride, acetonitrile, methanol, dimethylformamide (DMF), LC–MS-grade water and phosphate-buffered saline (PBS) were purchased from Fisher Scientific (NJ, USA). Rabbit antihuman antibodies to LAMP1, Rab7, Rab11, Rab14 and AlexaFluor 488 conjugated goat antirabbit IgG were purchased from Santa Cruz Biotechnology (TX, USA). Folate-modified P407 (FA-P407) and CF633-modified P407 were synthesized as described [20].

MABC synthesis

ABC (3.49 mmol, 1 equivalent) was dried by azeotroping from anhydrous pyridine, then suspended in anhydrous DMF and cooled to 0°C under argon. Selective silylation of the 5-hydroxyl group of ABC was conducted by adding *tert*-butyldimethylsilyl chloride (4.18 mmol, 1.2 equivalents) and imidazole (5.23 mmol, 1.5 equivalents) to the suspension with continuous stirring for 16 h after which the desired silylated product was isolated by flush chromatography purification and characterized by proton nuclear magnetic resonance (^{1}H-NMR) spectroscopy. The amino group in the silylated ABC was then protected by reacting with DMTr-Cl (5.05 mmol, 2.2 equivalents) in anhydrous pyridine solvent to yield orthogonally protected ABC. Selective cleavage of the silyl group was achieved using tetra-*n*-butylammonium fluoride (4.87 mmol, 2.5 equivalents) to afford the free primary alcohol that was coupled with myristic acid (3.36 mmol, 2 equivalents) using 1-[bis(dimethylamino) methylene]-1H-1,2,3-triazolo[4,5-b]pyridinium 3-oxid hexafluorophosphate (3.63 mmol, 2.2 equivalents) and *N,N*-diisopropylethylamine (8.26 mmol, 5 equivalents) in DMF. Finally, cleavage of DMTr using trifluoroacetic acid produced MABC after purification; ^{1}H-NMR spectrum specifics: R_f 0.38 (9:1 CH_2Cl_2/MeOH); ^{1}H-NMR (500 MH*z*, CD_3OD) δ 0.60–0.67 (br, 2H), 0.82–0.94 (m, 5H), 1.21–1.50 (br, 23H), 1.69–1.80 (m, 3H), 2.60–2.74 (br, 1H), 2.82 (t, J = 8.6 H*z*, 1H), 2.85 (t, J = 8.6 H*z*, 1H), 2.96–3.12 (br, 2H), 3.61 (dd, J = 5.3, 10.8 H*z*, 1H), 3.68 (dd, J = 5.3, 10.8 H*z*, 1H), 5.77–5.80 (br, 1H), 5.92–5.98 (m, 1H), 6.16–6.33 (m, 1H), 8.01 (s, 1H).

Antiretroviral activity of MABC

Human peripheral blood monocytes were obtained from HIV-1 and -2 and hepatitis seronegative donors and purified using countercurrent centrifugal elutriation [28]. The monocytes were cultured and differentiated into macrophages (monocyte-derived macrophages [MDMs]) using DMEM with 10% heat-inactivated pooled human serum, 1% glutamine, 50 µg/ml gentamicin, 10 µg/ml ciprofloxacin and 1000 U/ml macrophage colony stimulating factor (MCSF) for 7–10 days [29]. The antiviral activity of native drug and prodrug against HIV-1 was determined in human MDM at day 10 postinfection as described [30]. Briefly, MDM were exposed to various concentrations of ABC or MABC for 60 min followed by challenge with HIV-1_{ADA} at a multiplicity of infection (MOI) of 0.01 infectious viral particles per cell. After 4 h of incubation, cells were washed three-times with PBS to remove excess virus followed by incubation with the same concentration of drug used before

infection. Cells were cultured for an additional 10 days with half media changes every other day with equivalent replacement of drug containing media. Supernatants were collected at day 10 after viral infection, and the level of viral replication was determined by HIV reverse transcriptase (RT) activity [31].

Nanoformulated MABC

Crystalline MABC was encased in poloxamer P407 (nanoformulated MABC) using high-pressure homogenization (Avestin EmulsiFlexC3; Avestin, Inc., ON, Canada) [16,19]. For preparation of non-targeted nanoformulation (NMABC), a suspension of 1% (w/v) MABC and 0.5% (w/v) P407 in 10 mM HEPES buffer (pH 5.5; Sigma) was premixed overnight at room temperature to generate drug containing polymeric micelles. Suspensions were then homogenized by high-pressure homogenization (20,000 psi) until the desired particle size of approximately 250 nm was achieved. Folate-targeted nanoformulation (FA-NMABC) was prepared in an analogous manner from a premix of 0.5% polymer as FA-P407 and P407 (60:40% w/w) [20]. Crude nanoformulations were purified by differential centrifugation at 5000 × *g* for 5 min to remove aggregated particles. Further centrifugation at 20,000 × *g* for 20 min was used to remove the free MABC and polymeric micelles. Purified nanoparticle pellets were resuspended in 10 mM HEPES buffer (pH 5.5) for physicochemical characterization and for *in vitro* and *in vivo* studies. To prepare CF633-P407-labeled nanoformulations, CF633-P407 and P407 were dissolved in methanol at a weight ratio of 1:5 [20,32]. Methanol was then evaporated to generate a thin polymer film that was rehydrated using 10 mM HEPES buffer (pH 5.5) to yield a final excipient concentration of 0.5% (w/v). To this polymer solution, free MABC was added at a 1% (w/v) ratio. The suspension was protected from light and premixed at room temperature for 16 h. The suspension was homogenized and purified as described earlier for unlabeled formulations. CF633-labeled folate-targeted nanoformulations were prepared similarly where CF633-P407, P407 and FA-P407 were dissolved in methanol at a weight ratio of 1:2:2.

Physicochemical characterizations of MABC & its derivatives

MABC was characterized using ^{1}H-NMR and Fourier transform infrared (FTIR) spectroscopy. ^{1}H-NMR spectra were recorded on a Varian INOVA 500 MHz spectrometer (Varian, Inc., CA, USA). ^{1}H-NMR data is reported in ppm downfield from tetramethylsilane as an internal standard (IS). FTIR spectra were recorded using a Spectrum Two UATR-Two FTIR spectrometer (PerkinElmer, Inc., MA, USA). Nanoformulations were characterized for their particle size, polydispersity index (PDI) and ζ potential by dynamic light scattering (DLS) using a Malvern Zetasizer, Nano Series Nano-ZS (Malvern Instruments, Inc., MA, USA). The morphology of the nanoformulations was examined by scanning electron microscopy (SEM) using a Hitachi S4700 field-emission scanning electron microscope (Hitachi High Technologies America, Inc., IL, USA) [16]. Stability of the nanoformulation suspensions was assessed at room temperature (25°C) and at 4°C for a period of 8 weeks by measuring particle size and PDI by DLS. Drug loading, in other words, the weight percentage of MABC encapsulated in a given mass of lyophilized nanoformulation, was determined by ultraperformance LC–MS/MS (UPLC–MS/MS). To determine drug concentration in purified nanosuspensions, an aliquot of the nanosuspension was extracted using methanol and analyzed by UPLC–MS/MS [20].

Nanoparticle MDM uptake & retention

Uptake and retention of nanoformulations were determined in human MDM [16,33]. Briefly, MDM were treated with nanoformulations at a concentration of 100 µM MABC. Cell uptake was assessed at different time points without any media changes. At each time point, adherent MDM were washed three-times with 1 ml of PBS, scraped into 1 ml of fresh PBS and pelleted by centrifugation at 950 × *g* for 8 min. The cell pellet was reconstituted in 200 µl methanol and probe sonicated followed by centrifugation at 20,000 × *g* for 20 min. The supernatant was analyzed for drug content using UPLC–MS/MS.

To determine involvement of folate receptors (FOLR) in MDM uptake of the folate-targeted nanoformulation, cells were preincubated with 50 µM free FA for 60 min prior to treatment with 100 µM FA-NMABC. For cell retention studies, MDM were treated with 100 µM of nanoformulated MABC for 8 h; cells were then washed with PBS to remove free drug or unincorporated nanoparticles followed by further incubation in MCSF-free medium without nanoformulation. At days 1, 5, 10 and 15, cells were washed, collected and analyzed for drug content as described for uptake studies. Cell viability was determined using 3-(4,5-dimethylthiazol-2-yl)-2,5-diphenyltetrazolium bromide (MTT) [16]. Briefly, MDM were treated with 10, 50, 100 and 200 µM NMABC or FA-NMABC for 24 h. The adherent cells were washed with PBS, and 200 µl of MTT working solution (0.5 mg/ml diluted in MCSF-free media) was added to the cells followed by incubation at 37°C for 30 min and washing with PBS. DMSO (200 µl/well) was added to the cells and incubated for 5 min at 25°C. The absorbance

at 490 nm was measured using a SpectraMax M3 Microplate reader (Molecular Devices, CA, USA).

Antiretroviral activity of MABC nanoformulations

MDM were treated with 100 µM MABC using free MABC or nanoformulated MABC for 8 h. The cells were washed with PBS to remove excess free drug and nanoparticles. The MDM were challenged with HIV-1_{ADA} at an MOI of 0.01 infectious viral particles per cell for 18 h on day 1, 5, 10 and 15. Progeny virion production was measured by RT activity in culture medium [31]. HIV-1 p24 protein expression was assessed in adherent cells [32]. The cells were washed with PBS and fixed with 4% paraformaldehyde for 15 min at room temperature. The cells were blocked using 10% bovine serum albumin (BSA) containing 1% Triton X-100 in PBS for 30 min at room temperature. Following blocking, cells were incubated with HIV-1 p24 mouse monoclonal antibodies (1:50; Dako, CA, USA) for overnight at 4°C, followed by 1-h incubation at room temperature. Horseradish peroxidase (HRP)-labeled polymer antimouse secondary antibody (Dako EnVision® System; Dako) was added (one drop per well). Hematoxylin (500 µl/well) was added to counterstain the nuclei, and images were captured using a Nikon TE300 microscope with a 20× objective.

MABC nanoparticle subcellular localization

To determine subcellular localization of nanoformulated MABC, human monocytes were cultured in an eight-well Lab-Tek II CC2 chamber slide at a density of 5×10^5 cells/well and differentiated into macrophages as described previously [20]. MDM were treated with 100 µM of MABC using CF633-labeled NMABC or FA-NMABC for 8 h, washed with PBS, fixed and stained using subcellular compartment antibodies [20,32]. Briefly, cells were fixed with 4% paraformaldehyde for 30 min at room temperature, permeabilized using 5% Triton-X in PBS for 15 min, and blocked with 5% BSA and 0.1% Triton-X in PBS. The cells were then incubated overnight at 4°C for 1 h at room temperature with primary antibody (1:25 dilution in 5% BSA and 0.1% Triton-X in PBS) for respective endocytic compartments: late endosomes (Rab 7; sc-10767), recycling endosomes (Rab11 and Rab14; sc-9020 and sc98610) and lysosomes (LAMP1; sc-5570). The cells were washed extensively using 0.1% Triton-X in PBS and subsequently were incubated with secondary antibody conjugated with AlexaFluor 488 for 60 min at room temperature. The cells were covered with ProLong Gold anti-fade reagent with DAPI I (4,6-diamidino-2-phenylindole), cover slipped and imaged by confocal microscopy using an LSM 510 microscope with a 63× oil lens (Carl Zeiss Microimaging, Inc., CA, USA).

PK studies

Animal PK studies were conducted in accordance with the University of Nebraska Medical Center Institutional Animal Care and Use Committee. Male Balb/cJ mice (Jackson Labs, ME, USA) were maintained on a folate-deficient diet (Harlan Teklad TD.00434; Harlan Laboratories, Inc., IN, USA) for two weeks prior to treatment and throughout the study. Mice were injected intramuscularly with 50 mg/kg ABC equivalents using native ABC, NMABC or FA-NMABC in PBS. On days 1, 3, 5, 7, 9, 12 and 14 after drug treatment approximately 50 µl blood was collected by cheek bleeding, and immediately 40 µl was added into 1 ml of acetonitrile for drug analysis. IS (10 µl) was added to each sample and consisted of 0.665 µg/ml d_4-ABC and 0.5 µg/ml lopinavir. Samples were centrifuged at 17,000 × *g* for 10 min, and supernatants were dried using a ThermoScientific Savant Speed Vacuum (ThermoScientific, MA, USA), reconstituted in 100 µl of 80% v/v methanol in LC–MS-grade water and 10 µl was injected directly for MABC UPLC–MS/MS analysis. About 30 µl of the reconstituted samples were diluted with 50 µl water for ABC UPLC–MS/MS analysis. Final concentrations for both d_4-ABC (IS for ABC) and lopinavir (IS for MABC) were 50 ng/ml. Standard curves of ABC or MABC were prepared similarly, in blood collected from control mice in the range of 0.35–3500 and 0.125–1250 ng/ml, respectively. A Waters ACQUITY H-class UPLC system (Waters, MA, USA) connected to a Waters Xevo TQS-micro mass spectrometer with an ESI source was used for drug quantitation. Chromatographic separation of 10 µl ABC sample injections was achieved on an ACQUITY UPLC CSH C18 column (1.7 µm, 100 mm × 2.1 mm) using a 13-min gradient of mobile phase A (7.5 mM ammonium bicarbonate in LC-MS-grade water, adjusted to pH 7 with glacial acetic acid) and mobile phase B (100% LC–MS-grade methanol) at a flow rate of 0.25 ml/min. The initial mobile phase composition was 10% B for the first 2.5 min and was gradually increased to 95% B in 6.5 min and held constant for 1.5 min. Mobile phase B was then reset to 10% in 0.45 min, and the column was equilibrated for 2.25 min before the next injection. MABC chromatographic separation was achieved using the same CSH C18 column and mobile phases but with a 16-min isocratic method using 81% mobile phase B and flow rate of 0.3 ml/min. ABC and MABC were detected at a cone voltage of 8 and 16 V, respectively, and a collision energy of 16 and 30 V, respectively, in the positive ionization mode. Multiple reaction monitoring tran-

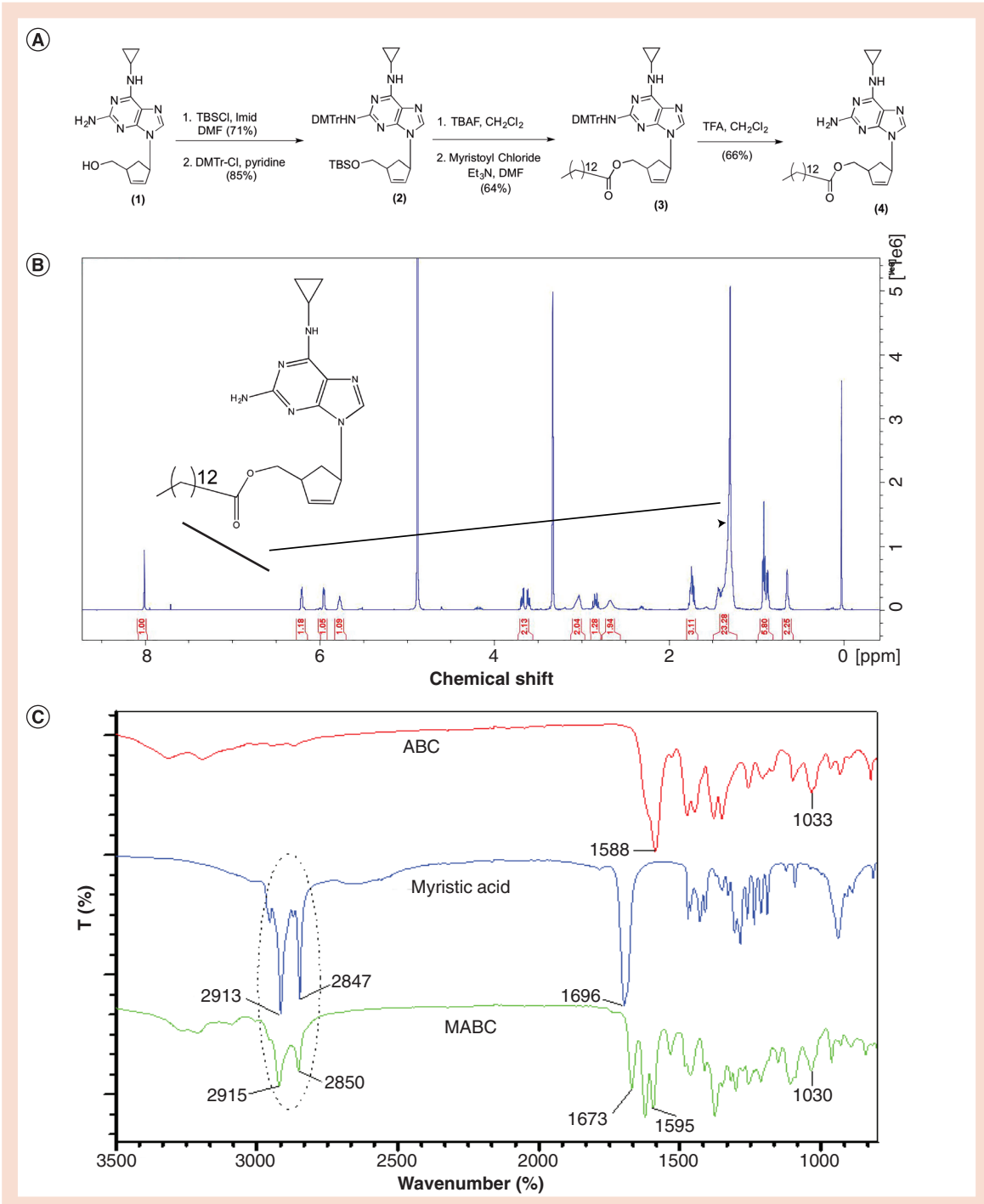

Figure 1. Synthesis and characterization of MABC (cont. overleaf). **(A)** MABC was synthesized as illustrated at a final yield of 66%. **(B)** The ^{1}H-NMR spectrum of MABC showed the presence of an intense broad peak at 1.21–1.50 ppm. This peak corresponds to the aliphatic protons on the fatty acid moiety. **(C)** Peaks at 2915 cm^{-1} and 2850 cm^{-1} in MABC FTIR spectrum correspond to alkane (CH_2-CH_2) stretching of the myrisitic acid alkane. **(D)** The ^{1}H-NMR spectrum of NMABC showed the presence of a singlet at 3.7 ppm that corresponds to the methylene-repeating unit of the polymer. Peaks corresponding to the myristoylated prodrug protons are also displayed on the formulation spectrum.

sitions used for ABC, MABC, d_4-ABC and lopinavir were 287.14 > 191.00, 497.18 > 191.07, 291.14 > 79.02 and 629.18 > 447.2 (m/z), respectively. Spectra were analyzed and quantified by MassLynx software version 4.1. All calculations were made using analyte peak area to IS peak area ratios.

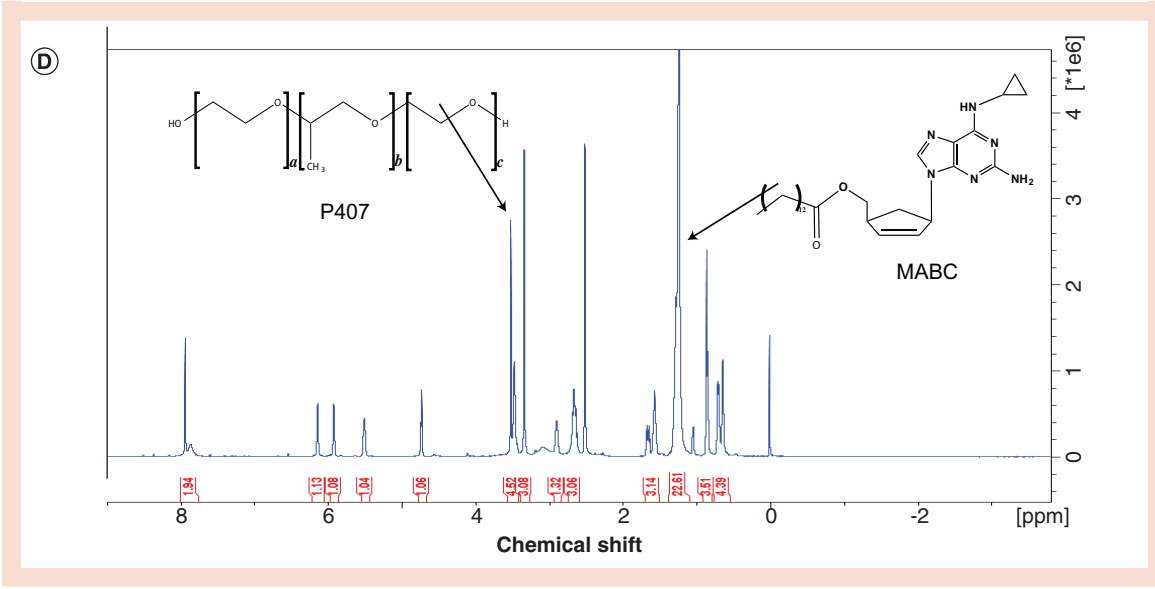

Statistical analyses

Drug uptake and retention data were analyzed by one-way analysis of variance and Student's *t*-test using GraphPad Prism software (GraphPad Software, Inc., CA, USA). Confocal images were analyzed as percent overlap using ImageJ software with JACoP plugin to quantify the amount of overlap between labeled nanoparticles and labeled endocytic compartments. Differences of mean percent overlap between nanoformulations were analyzed using Student's *t*-test. Experiments were performed three-times unless otherwise specified. Animal studies were conducted with five animals per treatment group. Statistical analysis was performed by two-way analysis of variance and Bonferroni's multiple comparison test. Results are expressed as mean ± standard error of mean. Results were considered significant at a p-value of <0.05.

Results

MABC synthesis & characterization

In its native form, ABC has restricted intracellular and tissue penetrance [30,34]. Its hydrophilic nature also poses challenges for nanoformulation preparations. To facilitate encapsulation of ABC into a poloxamer-stabilized nanosuspension, MABC, a hydrophobic prodrug of ABC, was synthesized. This was accomplished through derivatization of the native compound with a cleavable fatty acid ester (Figure 1A). Covalent linkage of myristic acid to the 5′-O-hydroxyl group of ABC was confirmed by ^{1}H-NMR, FTIR and MS/MS. Specifically, the triplet at 2.36 ppm in the ^{1}H-NMR spectrum of MABC represents two fatty acid methylene protons adjacent to the carbonyl group linked to ABC, while the broad multiplet signal in the region of 1.21–1.50 ppm of the spectrum corresponds to 20 hydrogens of the repeating methylene units of the fatty acid chain (Figure 1B). This was further confirmed by comparing FTIR spectra of MABC to that of native ABC and myristic acid (Figure 1C). The presence of alkane stretching (CH_2–CH_2) peaks at 2915 and 2850 cm^{-1} in the FTIR spectrum of MABC confirmed that the alkane chain of the derivatizing fatty acid (2913 and 2847 cm^{-1}) was covalently linked to the parent drug. The peaks at 1595 cm^{-1} in MABC and 1588 cm^{-1} in the ABC FTIR spectra corresponded to CH_2 stretching of the native aromatic ring. Peaks at 1673 and 1696 cm^{-1} in MABC and myristic acid corresponded to C=O fatty acid attachments. The peak at 1033 and 1030 cm^{-1} in ABC and MABC spectra corresponded to NH_2 vibrations of the parent compound. Infusion into a Waters Xevo TQS micro mass spectrometer confirmed a molecular mass ion of 496.2, which corresponds to ABC with one myristoyl group (data not shown).

Antiretroviral activity of MABC

The antiretroviral activities of MABC and native drug were compared in MDM. Various concentrations of ABC or MABC bracketing the EC_{50} for ABC were added to MDM prior to and continued with HIV-1_{ADA} infection [30]. Antiretroviral activity was determined by measuring RT activity in culture fluids collected 10 days after drug treatment and infection. The antiviral activity of MABC as determined by the EC_{50} for viral suppression was comparable to that of the parent drug (~100 µM) (Figure 2).

Preparation & physicochemical characterization of the NMABC

Poloxamer nanoformulations of MABC were prepared by high-pressure homogenization as previously

described [16,18]. Nanoparticles in suspension were characterized by DLS and SEM. The physicochemical parameters of NMABC and FA-NMABC nanoparticles were similar. The size, PDI and ζ potential of NMABC nanoparticles were 160 ± 10 nm, 0.2 ± 0.1 and -27.5 ± 2.5 mV, respectively. Similarly, the size, PDI and ζ potential of FA-NMABC nanoparticles were 170 ± 12 nm, 0.15 ± 0.04 and -33.7 ± 3.7 mV, respectively. Relatively low PDI values displayed by the two nanoformulations indicated a narrow particle size distribution within the suspensions. Morphologically, both NMABC and FA-NMABC were observed to be cylindrical rods of 200 nm in size as determined by SEM, correlating with particle size determined by DLS (Figure 3A & B). The stability of nanoformulations over time and temperature was assessed by measuring the NMABC particle sizes over a period of 8 weeks at 4 and 25°C. During this time, the size and PDI did not change significantly at either of the two temperatures (Figure 3C & D), an indication that the nanoformulations remained stable for at least 2 months. Drug loading for NMABC and FA-NMABC nanoformulations was found to be 62 ± 1.5 and 65 ± 2.4% respectively. Lyophilized formulation powders were also characterized by magnetic resonance spectroscopy in DMSO. The presence of a singlet at 3.7 ppm in the ^{1}H-NMR spectrum of the formulation corresponds to the repeating methylene units (next to oxygen) of the polymer. Peaks corresponding to the myristoylated prodrug protons were also evident in the formulation spectrum.

Nanoformulated drug uptake & retention

To determine whether FOLR targeting would enhance MDM uptake and consequently retention of MABC, MDM were treated with 100 µM MABC using NMABC or FA-NMABC for up to 8 h. MDM uptake of nanoformulated MABC increased over time and reached a maximum at 8 h. As shown in Figure 4A, an up to 2.5-fold increase in uptake was observed for FA-NMABC compared with NMABC. Cell MABC concentrations for FA-NMABC nanoformulations were 5.12 ± 0.2, 11.3 ± 0.3, 19.07 ± 1.2 and 24.7 ± 1.5 µg per 10^6 cells at 1, 2, 4 and 8 h, compared with 2.1 ± 0.1, 3.5 ± 0.2, 8.6 ± 1.2 and 11.3 ± 1.5 µg per 10^6 cells for NMABC formulations at the same time points. In order to deduce whether improved uptake of FA-NMABC was mediated by the FOLR, MDM were incubated with excess free FA (50 µM) prior to treatment. As shown in Figure 4A, blocking FOLR with excess FA decreased FA-NMABC uptake to levels similar to that of NMABC. Substantial (1.5–3 orders of magnitude) differences were observed in the extent of MABC retention in MDM over 15 days with FA-NMABC compared with NMABC, reflecting the initial enhanced uptake using the folate-targeted nanoformulation (Figure 4B). The uptake and retention of MABC using FA-NMABC were significantly greater than that observed for NMABC (Student's *t*-test, **p < 0.001). The concentration of nanoformulations used (100 µM) did not induce cell toxicity as determined by the MTT assay (data not shown).

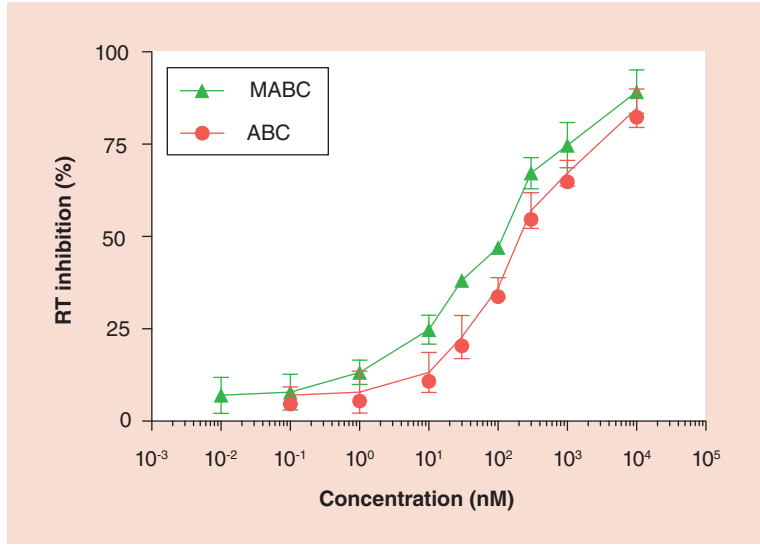

Figure 2. Antiviral activity of ABC and MABC in HIV-1_{ADA}-infected MDM. MDM were treated with various concentrations of ABC or MABC for 60 min and then challenged with HIV-1_{ADA} at a multiplicity of infection of 0.01 infectious viral particles/cell for 4 h. The cells were incubated for a further 10 days with MCSF-free media containing the same drug concentration. HIV RT activity was measured in the infectious supernatant on day 10 post-infection.

Antiretroviral activities of nanoformulated MABC

To determine whether improved hydrophobicity of MABC and subsequent improved uptake and retention in MDM using MABC nanoformulations would translate into improved antiretroviral activity, MDM were treated with 100 µM native ABC, free MABC, NMABC or FA-NMABC for 8 h. Following treatment, MDM were challenged with HIV-1_{ADA} at an MOI of 0.1 on days 1, 5, 10 and 15 post-treatment. Decreased RT activity in infectious supernatants collected on day 10 postinfection revealed that FA-NMABC exhibited enhanced antiretroviral activity compared with NMABC or free MABC (Figure 4C). RT activity was not decreased in supernatants collected from MDM treated with native ABC, suggesting either no uptake or rapid metabolism of the native drug. However, native ABC suppressed HIV RT activity by 100 and 95% when cells were treated 12 and 24 h after HIV-1 exposure (data not shown). HIV replication using FA-NMABC was suppressed by 100 ± 2.3% at days 1 and 5 and by 88 ± 3.4 and 70 ± 2.5% at days 10 and 15;

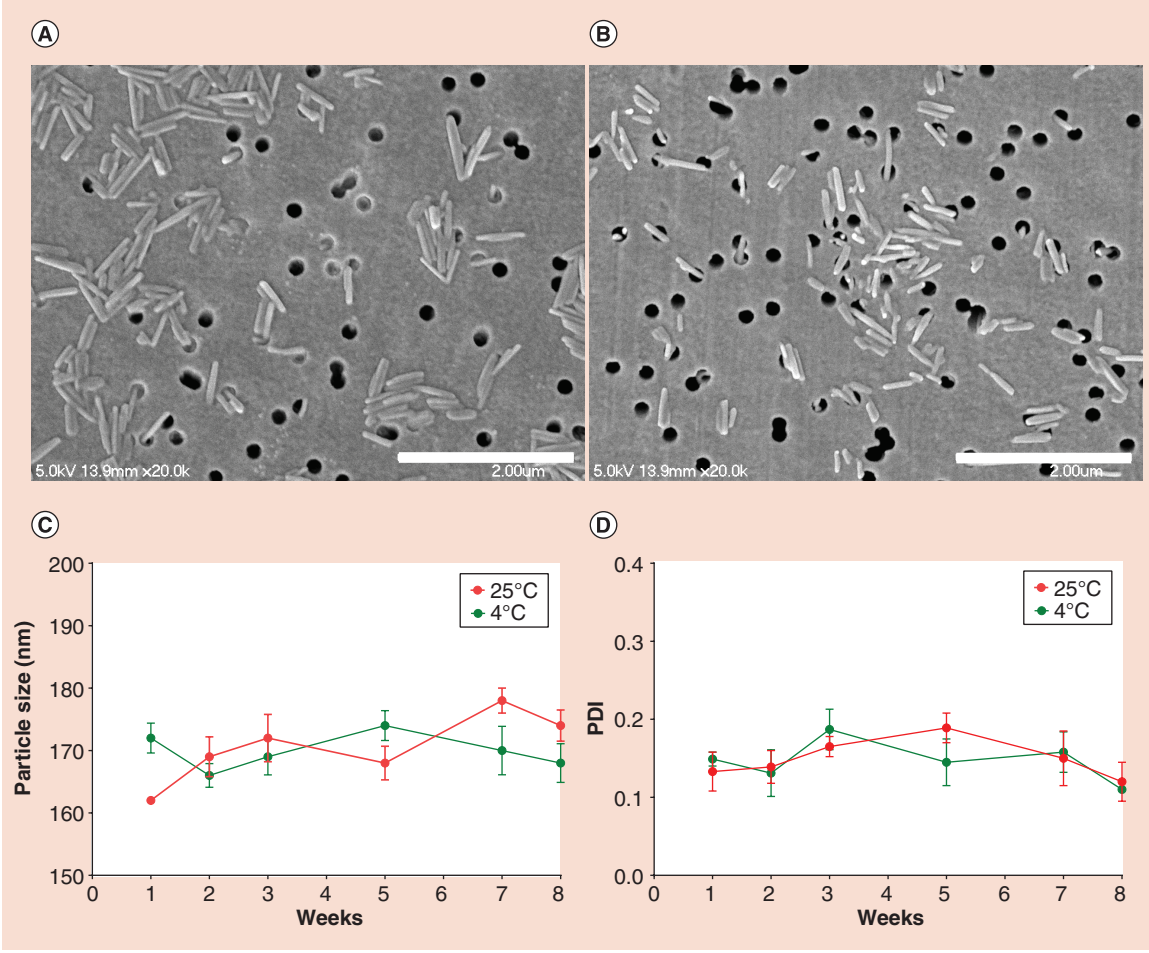

Figure 3. Morphology and stability of NMABC. SEM images of **(A)** NMABC and **(B)** FA-NMABC nanoformulations. Both formulations appeared as cylindrical monodispersed particles of ~200 nm. Stability of the NMABC nanoformulation was assessed by measuring **(C)** particle size and **(D)** PDI at 4°C and 25°C for 8 weeks.

whereas, NMABC suppressed viral replication by 100 ± 1.5, 78 ± 1.7, 72 ± 3.5 and 52 ± 4.5 at days 1, 5, 10 and 15, respectively. Minimal or no inhibition was achieved using free MABC (Figure 4C). RT activity was cross-validated by evaluating HIV-1 p24 antigen expression in adherent MDM 10 days postinfection. MDM treated with free MABC or NMABC showed increased viral infection from days 1 to 15, as observed by the intensity of brown staining of p24 antigen; whereas, minimal to no p24 antigen was detected in MDM treated with FA-NMABC measured at all time points (Figure 4D).

Subcellular nanoparticle localizations

Subcellular localization of the nanoformulations taken up by MDM was assessed using confocal microscopy. MDM were treated with 100 µM CF633-labeled NMABC or FA-NMABC for 8 h. Physicochemical parameters for CF633-labeled nanoformulations were similar to that of unlabeled nanoformulations (data not shown). After incubation, cells were washed, fixed and stained with antibodies to endosomal compartments as described [20,32]. Rab7 antibody identified the late endosomal compartments; Rab11 and Rab14 antibodies identified compartments involved in recycling; and LAMP1 (lysosomal-associated membrane protein 1) antibody identified the lysosomal compartments. Colocalization was seen as a yellow punctate pattern throughout the cytoplasm and perinuclear cell regions in the merged images of red nanoparticles and green compartments. For both nanoformulations colocalization was found predominantly in recycling endosomes compared with late endosomal and lysosomal compartments (Figure 5A). Percent overlap between endosomal compartments and nanoformulations, as determined using ImageJ software and JACoP plug-in, showed greater colocalization of nanoparticles with recycling endosomal compartments (46 ± 2.4 and 62 ± 1.5%, Rab11 and Rab14 for NMABC; 70 ± 1.7 and 79 ± 4.3, Rab11 and Rab14 for FA-NMABC) than with lysosomal and late endosomal compartments (27 ± 1.8 and 36 ± 2.3%, LAMP1 and Rab7 for NMABC;

34 ± 3.2 and 64 ± 2.8, LAMP1 and Rab7 for FA-NMABC) (Figure 5B). FA-NMABC exhibited significantly greater colocalization with all compartments compared with NMABC.

PK studies

To determine whether improved hydrophobicity and encapsulation of MABC into poloxamer nanoformulations would translate into sustained blood ABC drug levels *in vivo*, mice were injected intramuscularly with 50 mg/kg of native ABC or an equivalent ABC dose as NMABC or FA-NMABC. Mice have approximately tenfold higher free folate levels than humans, and excess folate may block the FOLR and interfere with rapid uptake of folate-targeted nanoformulation [35]. Thus, prior to treatment, mice were placed on folate-deficient diet for 2 weeks to reduce plasma folate levels [18]. For ABC and MABC analyses, whole blood was collected immediately into acetonitrile to inhibit the activity of esterases, which would cleave the myristoyl group from MABC, and adenosine deaminase, which could convert ABC to carbovir [30]. ABC blood levels measured at days 1, 3, 5, 7, 9, 12 and 14 post-treatment were significantly higher in mice treated with FA-NMABC compared with those treated with NMABC or native ABC. This was reflected in higher ABC levels (2.6–4.9-fold) in lymphoreticular tissues (liver, spleen and lymph nodes) in mice treated with nanoformulated MABC compared with native ABC (Supplementary Figure). MABC was lower than the limit of quantitation (<0.125 ng/ml) in all samples, indicating rapid conversion of the MABC to ABC in blood and tissues. By day 14, ABC blood levels were 36 ± 4.7, 21 ± 3.8 ng/ml and below the limit of quantitation (0.5 ng/ml) in mice treated with FA-NMABC, NMABC and native drug, respectively (Figure 6).

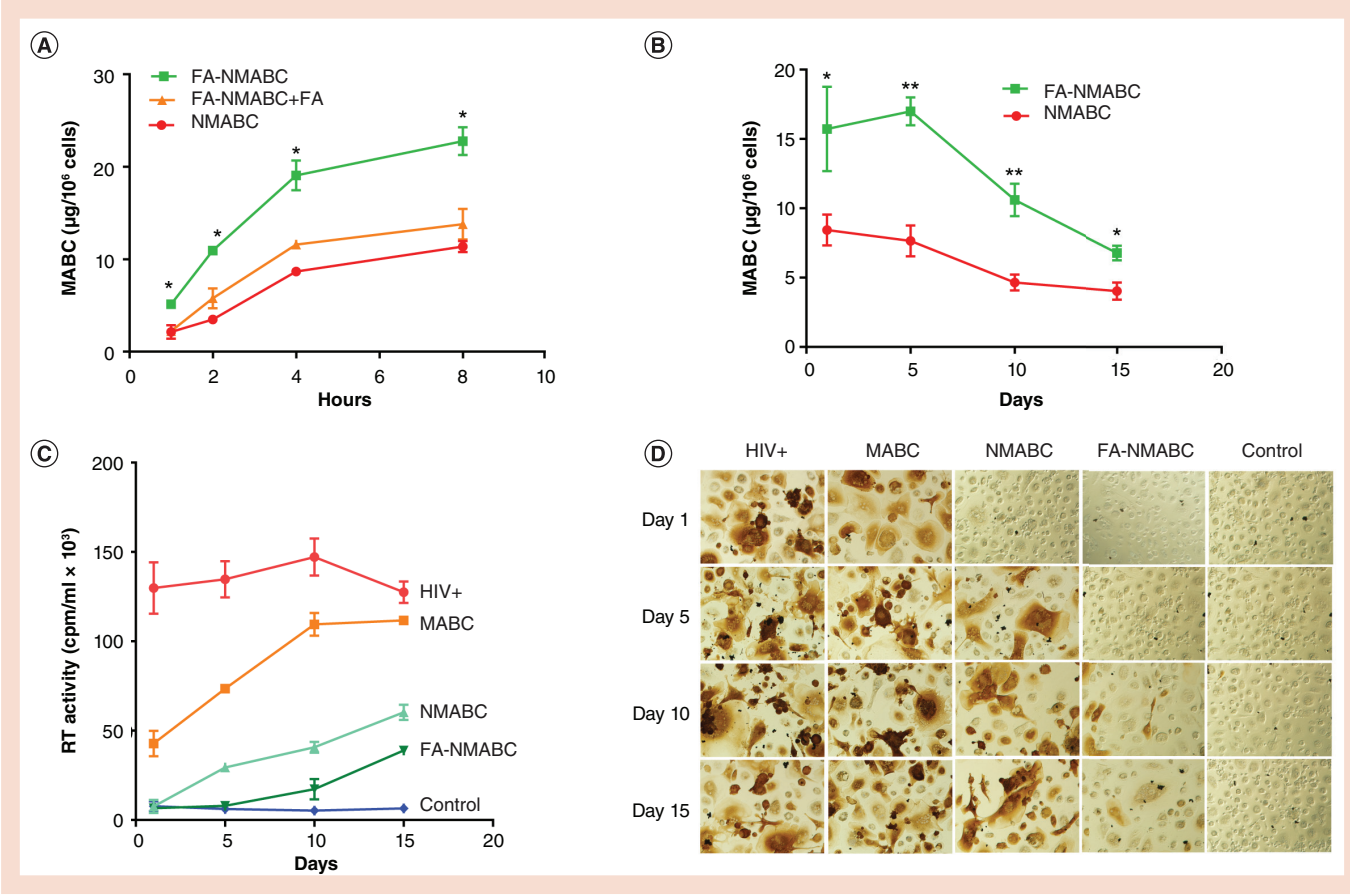

Figure 4. MDM uptake, retention and antiviral activity of NMABC and FA-NMABC. (A) MDM uptake of 100 µM NMABC or FA-NMABC was determined over 8 h. For uptake studies, 50 µM free folic acid (FA) was added to MDM prior to treatment with FA-NMABC to block FOLR binding. **(B)** MDM retention of NMABC or FA-NMABC was determined over 15 days. Antiretroviral activity was determined in MDM treated for 8 h with 100 µM free MABC or nanoformulated MABC and then infected with HIV-1_{ADA} at 1, 5, 10 or 15 days following drug loading. HIV replication was determined 10 days after infection by **(C)** HIV RT activity and **(D)** HIV p24 staining. For uptake studies, statistical differences were determined using one-way ANOVA among three groups; for retention studies statistical differences were determined using Student's *t*-test.
*p < 0.05; **p < 0.001.

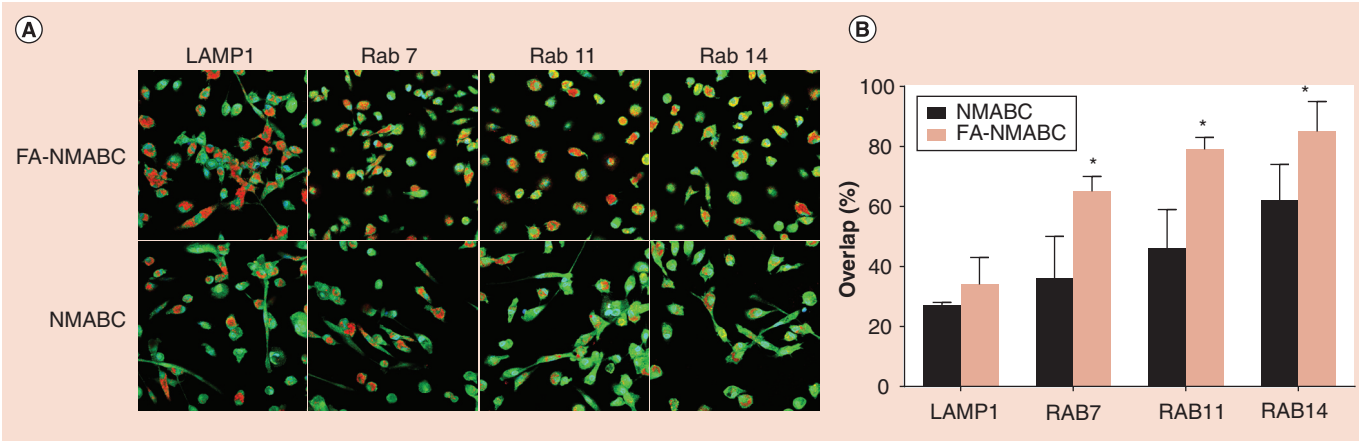

Figure 5. Subcellular localization of nanoformulated MABC in MDM. MDM cultured in 8 well Lab-Tek II CC² chamber slides were treated with 100 μM CF633-labeled FA-NMABC or CF633-labeled NMABC for 8 h then fixed and stained with antibodies to Rab7, -11, -14, and LAMP1 as described [20]. **(A)** Co-localization is observed as a yellow punctate pattern throughout the cytoplasm and perinuclear cell regions in merged images of red nanoparticles and green subcellular compartments. **(B)** Percent fluorescence overlap was quantitated using ImageJ software and JACoP plug-in. Statistical differences were determined using Student's *t*-test.
*p < 0.05.

Discussion

Currently, the nucleoside reverse transcriptase inhibitor (NRTI) ABC is recommended as a component of a first-line treatment regimen by the National AIDS Control Organization [36]. In combination with two other NRTIs, for example, zidovudine and lamivudine (3TC) such as Trizivir, it is part of a three-drug antiretroviral regimen [36,37]. Notably, viral strains that are resistant to zidovudine or 3TC can be sensitive to ABC [38]. However, ABC is associated with a dose-dependent hypersensitivity response that may lead to death if therapy is not discontinued, and patients must be prescreened for the *HLA-B*5701* allele [39]. ABC can be used as an alternative to Truvada in pre-exposure prophylaxis drug regimens used in the management of HIV-1 transmission [40,41]. Trizivir and other combination therapies lead to decreased viral resistance and improved long-term survival. Currently, ABC, 3TC and dolutegravir are recommended as the most effective ART regimen [42]. However, the short half-lives of the current regimens and the intrinsic physicochemical properties of these antiretroviral drugs have limited their utilities and hence demonstrate the need for long-acting delivery platforms that can improve patient adherence and facilitate drug entry into restricted anatomical reservoirs of HIV-1 persistence [15]. While progress has occurred toward developing long-acting nanoformulations for protease and non-nucleoside RT inhibitors [16,19,20,43] development of nanoformulations of hydrophilic drugs has remained elusive. Attempts have been made to encapsulate ABC into polymeric nanomedicines but poor loading and fast release kinetics have hampered their clinical applicability [44].

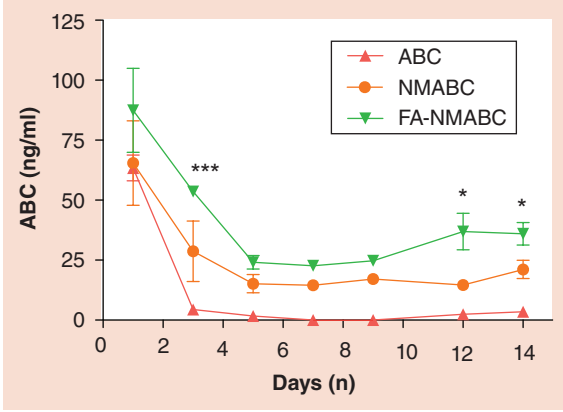

Figure 6. Blood drug levels of nanoformulated MABC in mice. Balb/c mice were administeredintramuscularly 50 mg /kg equivalents of ABC using free ABC, NMABC or FA-NMABC on day 0 and sacrificed on day 14. Whole blood was collected into acetonitrile for drug analysis on days 1, 3, 5, 7, 9, 12, and 14 after treatment. ABC levels were determined by UPLC-MS/MS. Data are expressed as mean ± standard error of mean.
*p < 0.05; ***p < 0.0001; statistically different from ABC as determined by 2-way ANOVA and Bonferroni's Multiple Comparison tests.

To overcome such challenges, a carboxylic acid ester prodrug approach has been widely used to improve lipophilicity and oral absorption of nucleoside analogs [23,45]. In this approach, a carboxylic acid containing hydrophobic alkyl chain is reacted with the hydroxyl group located at the five-membered ring moiety of the nucleoside analog. Even though the carboxylic acid ester prodrug approach has been used to modify a variety of anticancer compounds [46,47] and antiviral drugs [48], development and nanoformulation of hydrophobic derivatives of antiretroviral drugs such as 3TC and ABC remain elusive. The goal of the

present study was to improve the half-life and therapeutic efficacy of ABC through derivatization of the highly water soluble parent drug with a hydrophobic fatty acid side chain to generate a myristoylated prodrug that would be easily encapsulated into polymer excipients and other surfactants to target macrophages. The 5-hydroxyl group on the cyclopentene moiety of ABC was esterified with myristic acid, a 14 carbon chain fatty acid. MABC was successfully synthesized at a final yield of 66% after purification and characterized using ^{1}H-NMR and FTIR spectroscopy. In the cell, MABC was converted to ABC by esterase cleavage followed by phosphorylation to produce the therapeutically active compound [30]. The success of such a strategy has been shown for CP-4126, a fatty acid prodrug of gemcitabine, which upon cleavage by esterases resulted in a 200-fold increase in therapeutic activity [46]. Our results demonstrated that prodrug synthesis does not impair the antiretroviral activity of parent ABC, as determined by RT activity.

Over the past decade, work from our laboratory has demonstrated the potential of targeted nanoART to produce sustained high plasma and tissue drug concentrations for weeks following a single intramuscular administration that can suppress ongoing viral replication and mitigate dose associated viral resistance [17,19]. In this context, nanoART was manufactured using folate-conjugated P407 that targets the FOLR2 expressed on activated macrophages [20]. Macrophage activation and subsequent overexpression of FOLR2 can be induced by folate-conjugated therapeutics [49]. Our results demonstrated that P407 and FA-P407 coating of MABC produced stable nanoformulations of similar physicochemical parameters. The drug loadings for both nanoformulations were high (62–65% w/w), which offers the advantage of administering a dose with less nonactive excipients. Since the geometry of nanoparticles plays an important role in determining the attachment to the macrophage surface [50], the morphology of the MABC nanoformulations was analyzed using SEM. Our results demonstrated that the morphology for both NMABC and FA-NMABC nanoparticles was cylindrical rods, which is advantageous in terms of macrophages uptake. The mechanism reflects the preference of macrophages for engulfment of most bacteria that have a rod-shaped geometry in nature [51].

In the case of folate targeting, receptor-mediated endocytosis occurs through interaction of FA moieties present on FA-nanoART with FOLR present on the macrophage surface [20]. Our results demonstrated that FA-NMABC nanoformulations showed a significantly increased macrophage uptake through binding to the FOLR compared with nontargeted NMABC. Indeed, folate-mediated uptake was cross-validated by the inhibition of FA-NMABC uptake by blocking the FOLR with excess free FA (Figure 4A). When FOLR were blocked, the uptake of FA-NMABC by MDM was significantly decreased to a level similar to that for NMABC demonstrating that the superior uptake of folate nanoformulations occurred through engagement of the FOLR. Consequently, the amount of MABC that was retained in MDM using FA-NMABC was greater compared with that for NMABC nanoformulations (Figure 4B). MDM retained more than twofold greater levels of FA-NMABC than NMABC over a period of 15 days. As a consequence of enhanced uptake and retention of MABC, the FA-NMABC nanoformulations exhibited superior antiretroviral activity compared with NMABC nanoformulations as measured by RT activity and HIV-1 p24 antigen staining (Figure 4C & D). The protection of MDM from HIV-1_{ADA} infection was observed for 15 days using folate-targeted nanoformulations, in contrast to reduction in protection by 5–10 days for nontargeted formulations and free drug. Thus, sustained drug delivery and improved antiretroviral activity of MABC might be expected *in vivo* using folate-coated nanoformulations. In addition, no cytotoxicity was observed in MDM at the nanoformulations concentration tested.

Our laboratory demonstrated previously that storage of nanoART in late or recycling endosomal compartments provides a protected environment for the encased cargo in the same subcellular organelles that harbors the pathogen and promotes slow release of the encapsulated drugs. Similar subcellular trafficking pathways for nanoparticles and HIV would enhance the antiretroviral response of the drugs [32,52]. In this study, subcellular localization of MABC nanoformulations was investigated in MDM. Our results showed greater colocalization of the MABC nanoformulations in recycling endosomal compartments (Rab11 and Rab14) compared with late endosomes (Rab7) or lysosomes (LAMP1) (Figure 5). For each compartment, the uptake of FA-NMABC was significantly higher compared with NMABC. These results reflect the higher overall uptake and greater antiviral efficacy of FA-NMABC compared with NMABC. However, some nanoparticles were localized in the degrading lysosomal compartments. Therefore, future studies will focus on minimizing the amount of nanoparticles trafficked into the lysosomal compartments to further improve the antiretroviral outcomes.

To determine whether FA-NMABC compared with NMABC or free drug could provide sustained blood drug levels, mice were treated with 50 mg/kg of ABC as free drug or MABC nanoformulations. Blood drug levels of ABC were detectable over 14 days following

treatment with nanoformulated MABC. The folate coating increased the blood levels of ABC by approximately 2.5-fold compared with noncoated formulations and up to 18-fold compared with native drug. Interestingly, no MABC was detected in the blood of mice treated with MABC nanoformulations. This suggests that following release from the nanoformulation, MABC was efficiently converted to ABC by blood and tissue esterases. Of particular interest, *in vivo* degradation of the prodrug results in release of ABC and myristic acid. Myristic acid has been shown to inhibit the activity of *N*-myristoyltransferase, a crucial enzyme that catalyzes myristoylation of several proteins involved in the life cycle of HIV [26,27]. This, in addition to increased protein binding of the prodrug, could result in improved efficacy of the myristoylated analog. Hence, folate coating of nanoformulated crystalline MABC could be an effective strategy to reduce HIV levels in its sanctuaries by maintaining sustained blood drug levels and through release of myristic acid.

The dose used in the present study (50 mg/kg) would translate into a 284-mg dose for a 70-kg adult by applying the US FDA guidelines scaling factor (animals to human equivalent dose conversion). The same dosing solution concentration used in mice (50 mg/ml) would translate to a 5.68-ml volume for delivery to a 70-kg adult. The nanoformulation suspension could be further concentrated to decrease the dose volume to effectively deliver in a single injection the current daily adult dose of 600 mg. Further extension of the half-life of long-acting antiretrovirals could be achieved through the use of adjunctive therapies such as URMC-099, which can enhance the macrophage storage capacity of these nanoformulations [53].

The issue of hypersensitivity is of critical concern for a long-acting formulation of ABC, but could be managed using *HLA-B*5701* testing as an accurate predictor for ABC hypersensitivity. In order to use the long-acting ABC in the clinical setting, three steps need to occur. First, *HLA-B*5701* testing would be required as an accurate predictor for ABC and all patients would be screened first to abrogate any likelihood of hypersensitivity reactions. Second, the patients would then be tested through oral drug administration for a period of up to 2 months to ensure there were no untoward reactions. Third, the patient would then be administered a single dose of long-acting medicines and following appropriate tolerance of the formulation the regimen would be continued long term [54].

Conclusion

We demonstrate that a carboxylic acid ester prodrug of ABC has improved antiretroviral activities over the native hydrophilic compound. The improved lipophilicity facilitated the encasement of the prodrug into poloxamer nanoformulations with high drug loading. Notably, coating the prodrug with a folate-modified polymer directed to the FA receptor enhanced nanoformulation uptake, retention and antiretroviral efficacy of the drug. MABC nanoformulations localized to recycling endosomal compartments in macrophages, as previously observed for nanoformulated atazanavir and ritonavir [32]. Of importance, following a single intramuscular injection, blood concentrations of ABC were maintained over 14 days using decorated nanoformulations.

Future perspective

We intend to improve the PK of our nanoformulated MABC using a range of particle surface ligands or through the use of mixed lineage kinase inhibitors that can affect autophagy and prolong the nanoparticle storage capacities. If successful, this would improve antiretroviral activities and facilitate MABC's use as a component in a long-acting ART regimen. Such strategies are now being tested in relevant mouse models of HIV/AIDS. Parallel development of a nanoformulated hydrophobic prodrug of 3TC would provide a combination drug regimen with MABC and a long-acting formulation of the integrase inhibitor dolutegravir. Future development of a combination long-acting prodrug-based delivery system would be a considerable benefit in the management of HIV infection.

Supplementary data

To view the supplementary data that accompany this paper please visit the journal website at: www.futuremedicine.com/doi/full/10.2217/nnm-2016-0164

Acknowledgements

The authors thank T Bronich for critical reading of the manuscript. They also thank JR Talaska and J Taylor of the Confocal Laser Scanning Core facility at the University of Nebraska Medical Center for assistance with confocal microscopy and the Scanning Electron Microscopy Core facility at the University of Nebraska-Lincoln for assistance with morphology analysis of nanoformulations.

Financial & competing interests disclosure

This work was supported by ViiV Healthcare and NIH grants P01 DA028555, R01 NS36126, P01 NS31492, 2R01 NS034239, P01 MH64570, P01 NS43985, P30 MH062261 and R01 AG043540. The authors have no other relevant affiliations or financial involvement with any organization or entity with a financial interest in or financial conflict with the subject matter or materials discussed in the manuscript apart from those disclosed.

No writing assistance was utilized in the production of this manuscript.

Ethical conduct of research

The authors state that they have obtained appropriate institutional review board approval or have followed the principles outlined in the Declaration of Helsinki for all human or animal experimental investigations. In addition, for investigations involving human subjects, informed consent has been obtained from the participants involved.

Executive summary

Myristoylated abacavir synthesis

- Modified abacavir (MABC) was synthesized by esterification of myristic acid to the 5-hydroxyl-cyclopentene moiety of the drug.
- MABC was recovered with 66% efficiency after purification.
- When compared with ABC, the antiretroviral activity of MABC was increased twofold in monocyte-derived macrophages.

Synthesis of MABC encased nanoformulations

- MABC was readily incorporated into P407-coated nanoparticles with a size range of 150–200 nm and a monodispersed cylindrical morphology.
- The nanoformulations were stable at 4 and 25°C for at least 8 weeks.

Pharmacokinetics evaluation of MABC nanoformulations

- Folate-targeting of the nanoformulation facilitated human monocyte-derived macrophages uptake and retention, and improved antiretroviral efficacy when compared with NMABC and free MABC.
- Macrophage drug depots were localized in recycling endosomes (Rab11 and Rab14).
- Following a single intramuscular injection of NMABC or FA-NMABC in mice, blood concentrations of ABC were maintained over 14 days.
- FA-NMABC enhanced blood drug levels in mice by 1.7-fold compared with NMABC.

References

Papers of special note have been highlighted as: • of interest; •• of considerable interest

1 Pirrone V, Thakkar N, Jacobson JM, Wigdahl B, Krebs FC. Combinatorial approaches to the prevention and treatment of HIV-1 infection. *Antimicrob. Agents Chemother.* 55(5), 1831–1842 (2011).

2 Chesney M. Adherence to HAART regimens. *AIDS Patient Care STDs* 17(4), 169–177 (2003).

3 Looney D, Ma A, Johns S. HIV therapy-the state of art. *Curr. Top. Microbiol. Immunol.* 389, 1–29 (2015).

4 Chun TW, Moir S, Fauci AS. HIV reservoirs as obstacles and opportunities for an HIV cure. *Nat. Immunol.* 16(6), 584–589 (2015).

5 Lorenzo-Redondo R, Fryer HR, Bedford T *et al.* Persistent HIV-1 replication maintains the tissue reservoir during therapy. *Nature* 530(7588), 51–56 (2016).

• **Identifies the key reservoirs established by HIV-1 during acute infection, and reasons why therapy failed.**

6 Massanella M, Fromentin R, Chomont N. Residual inflammation and viral reservoirs: alliance against an HIV cure. *Curr. Opin. HIV AIDS* 11(2), 234–241 (2016).

7 Fois AF, Brew BJ. The potential of the CNS as a reservoir for HIV-1 infection: implications for HIV eradication. *Curr. HIV/AIDS Rep.* 12(2), 299–303 (2015).

8 Giacalone G, Hillaireau H, Fattal E. Improving bioavailability and biodistribution of anti-HIV chemotherapy. *Eur. J. Pharm. Sci.* 75, 40–53 (2015).

9 Li JZ, Paredes R, Ribaudo HJ *et al.* Low-frequency HIV-1 drug resistance mutations and risk of NNRTI-based antiretroviral treatment failure: a systematic review and pooled analysis. *JAMA* 305(13), 1327–1335 (2011).

10 Swenson LC, Min JE, Woods CK *et al.* HIV drug resistance detected during low-level viraemia is associated with subsequent virologic failure. *AIDS* 28(8), 1125–1134 (2014).

11 Vyas TK, Shah L, Amiji MM. Nanoparticulate drug carriers for delivery of HIV/AIDS therapy to viral reservoir sites. *Expert Opin. Drug Deliv.* 3(5), 613–628 (2006).

• **Expert opinion on nanotherapeutic strategy for HIV/AIDS.**

12 Kumar P, Lakshmi YS, C B, Golla K, Kondapi AK. Improved safety, bioavailability and pharmacokinetics of Zidovudine through lactoferrin nanoparticles during oral administration in rats. *PLoS One* 10(10), e0140399 (2015).

13 Shegokar R, Singh KK. Surface modified nevirapine nanosuspensions for viral reservoir targeting: *in vitro* and *in vivo* evaluation. *Int. J. Pharm.* 421(2), 341–352 (2011).

14 Zhang T, Zhang C, Agrahari V, Murowchick JB, Oyler NA, Youan BB. Spray drying tenofovir loaded mucoadhesive and pH-sensitive microspheres intended for HIV prevention. *Antiviral Res.* 97(3), 334–346 (2013).

15 Spreen WR, Margolis DA, Pottage JC Jr. Long-acting injectable antiretrovirals for HIV treatment and prevention. *Curr. Opin. HIV AIDS* 8(6), 565–571 (2013).

16 Nowacek AS, Miller RL, Mcmillan J *et al.* NanoART synthesis, characterization, uptake, release and toxicology for

human monocyte-macrophage drug delivery. *Nanomedicine (Lond.)* 4(8), 903–917 (2009).

•• **Comprehensively introduces the synthesis of nanoformulated antiretroviral therapy (nanoART) followed by *in vitro* studies.**

17 Dash PK, Gendelman HE, Roy U *et al.* Long-acting nanoformulated antiretroviral therapy elicits potent antiretroviral and neuroprotective responses in HIV-1-infected humanized mice. *AIDS* 26(17), 2135–2144 (2012).

18 Gautam N, Puligujja P, Balkundi S *et al.* Pharmacokinetics, biodistribution, and toxicity of folic acid-coated antiretroviral nanoformulations. *Antimicrob. Agents Chemother.* 58(12), 7510–7519 (2014).

• **Pharmacokinetic study of nanoART in humanized mice.**

19 Puligujja P, Balkundi SS, Kendrick LM *et al.* Pharmacodynamics of long-acting folic acid-receptor targeted ritonavir-boosted atazanavir nanoformulations. *Biomaterials* 41, 141–150 (2015).

• **Pharmacodynamics of targeted nanoART.**

20 Puligujja P, Mcmillan J, Kendrick L *et al.* Macrophage folate receptor-targeted antiretroviral therapy facilitates drug entry, retention, antiretroviral activities and biodistribution for reduction of human immunodeficiency virus infections. *Nanomedicine* 9(8), 1263–1273 (2013).

•• **Describes the development of macrophage folate receptor-targeted antiretroviral therapy.**

21 Mahajan SD, Aalinkeel R, Law WC *et al.* Anti-HIV-1 nanotherapeutics: promises and challenges for the future. *Int. J. Nanomedicine* 7, 5301–5314 (2012).

22 Nowacek AS, Balkundi S, Mcmillan J *et al.* Analyses of nanoformulated antiretroviral drug charge, size, shape and content for uptake, drug release and antiviral activities in human monocyte-derived macrophages. *J. Control. Release* 150(2), 204–211 (2011).

23 Agarwal HK, Chhikara BS, Hanley MJ, Ye G, Doncel GF, Parang K. Synthesis and biological evaluation of fatty acyl ester derivatives of (-)-2',3'-dideoxy-3'-thiacytidine. *J. Med. Chem.* 55(10), 4861–4871 (2012).

24 Farazi TA, Waksman G, Gordon JI. The biology and enzymology of protein *N*-myristoylation. *J. Biol. Chem.* 276(43), 39501–39504 (2001).

25 Wu Z, Alexandratos J, Ericksen B, Lubkowski J, Gallo RC, Lu W. Total chemical synthesis of *N*-myristoylated HIV-1 matrix protein p17: structural and mechanistic implications of p17 myristoylation. *Proc. Natl Acad. Sci. USA* 101(32), 11587–11592 (2004).

26 Ohta H, Takamune N, Kishimoto N, Shoji S, Misumi S. *N*-Myristoyltransferase 1 enhances human immunodeficiency virus replication through regulation of viral RNA expression level. *Biochem. Biophys. Res. Commun.* 463(4), 988–993 (2015).

27 Takamune N, Hamada H, Misumi S, Shoji S. Novel strategy for anti-HIV-1 action: selective cytotoxic effect of *N*-myristoyltransferase inhibitor on HIV-1-infected cells. *FEBS Lett.* 527(1–3), 138–142 (2002).

28 Meltzer MS, Gendelman HE. Effects of colony stimulating factors on the interaction of monocytes and the human immunodeficiency virus. *Immunol. Lett.* 19(3), 193–198 (1988).

29 Dou H, Destache CJ, Morehead JR *et al.* Development of a macrophage-based nanoparticle platform for antiretroviral drug delivery. *Blood* 108(8), 2827–2835 (2006).

30 Balzarini J, Aquaro S, Hassan-Abdallah A, Daluge SM, Perno CF, Mcguigan C. Improved antiviral activity of the aryloxymethoxyalaninyl phosphoramidate (APA) prodrug of abacavir (ABC) is due to the formation of markedly increased carbovir 5'-triphosphate metabolite levels. *FEBS Lett.* 573(1–3), 38–44 (2004).

• **Explains the metabolic pathway of abacavir and provides insight into the metabolites-associated side effects.**

31 Kalter SS, Heberling RL, Barry JD, Kuramoto IK, Holland PV, Sazama K. Detection of antibody to immunodeficiency viruses by dot immunobinding assay. *J. Clin. Microbiol.* 30(4), 993–995 (1992).

32 Guo D, Zhang G, Wysocki TA *et al.* Endosomal trafficking of nanoformulated antiretroviral therapy facilitates drug particle carriage and HIV clearance. *J. Virol.* 88(17), 9504–9513 (2014).

•• **Introduces the concept that similar subcellular trafficking pathways for nanoparticles and HIV would enhance the antiretroviral response of the drugs.**

33 Balkundi S, Nowacek AS, Veerubhotla RS *et al.* Comparative manufacture and cell-based delivery of antiretroviral nanoformulations. *Int. J. Nanomedicine* 6 3393–3404 (2011).

34 Mcguigan C, Harris SA, Daluge SM *et al.* Application of phosphoramidate pronucleotide technology to abacavir leads to a significant enhancement of antiviral potency. *J. Med. Chem.* 48(10), 3504–3515 (2005).

35 Leamon CP, Reddy JA, Dorton R *et al.* Impact of high and low folate diets on tissue folate receptor levels and antitumor responses toward folate-drug conjugates. *J. Pharmacol. Exp. Ther.* 327(3), 918–925 (2008).

36 Adetokunboh OO, Schoonees A, Balogun TA, Wiysonge CS. Efficacy and safety of abacavir-containing combination antiretroviral therapy as first-line treatment of HIV infected children and adolescents: a systematic review and meta-analysis. *BMC Infect. Dis.* 15, 469 (2015).

• **Comprehensive study on the efficacy and safety of abacavir.**

37 Ibbotson T, Perry CM. Lamivudine/zidovudine/abacavir: triple combination tablet. *Drugs* 63(11), 1089–1098; discussion 1099–1100 (2003).

38 Wang LH, Chittick GE, McDowell JA. Single-dose pharmacokinetics and safety of abacavir (1592U89), zidovudine, and lamivudine administered alone and in combination in adults with human immunodeficiency virus infection. *Antimicrob. Agents Chemother.* 43(7), 1708–1715 (1999).

39 Hughes CA, Foisy MM, Dewhurst N *et al.* Abacavir hypersensitivity reaction: an update. *Ann. Pharmacother.* 42(3), 387–396 (2008).

• **Describes the side effects of abacavir.**

40 Van Damme L, Corneli A, Ahmed K *et al.* Preexposure prophylaxis for HIV infection among African women. *N. Engl. J. Med.* 367(5), 411–422 (2012).

41 Grant RM, Lama JR, Anderson PL *et al.* Preexposure chemoprophylaxis for HIV prevention in men who have sex with men. *N. Engl. J. Med.* 363(27), 2587–2599 (2010).

42 Pialoux G, Marcelin A, Cawston H *et al.* Cost–effectiveness of dolutegravir/abacavir/lamivudine in HIV-1 treatment naive patients in France. *Value Health* 18(7), A587 (2015).

43 Meng J, Zhang T, Agrahari V, Ezoulin MJ, Youan BB. Comparative biophysical properties of tenofovir-loaded, thiolated and nonthiolated chitosan nanoparticles intended for HIV prevention. *Nanomedicine (Lond.)* 9(11), 1595–1612 (2014).

44 Wilson B, Paladugu L, Priyadarshini SR, Jenita JJ. Development of albumin-based nanoparticles for the delivery of abacavir. *Int. J. Biol. Macromol.* 81 763–767 (2015).

45 Zhang Y, Gao Y, Wen X, Ma H. Current prodrug strategies for improving oral absorption of nucleoside analogues. *Asian J. Pharm. Sci.* 9(2), 65–74 (2014).

46 Bergman AM, Adema AD, Balzarini J *et al.* Antiproliferative activity, mechanism of action and oral antitumor activity of CP-4126, a fatty acid derivative of gemcitabine, in *in vitro* and *in vivo* tumor models. *Invest. New Drugs* 29(3), 456–466 (2011).

•• **Introduces the carboxylic acid ester prodrug approach to improve progressive lipophilicity and oral absorption of nucleoside analogs.**

47 Bergman AM, Kuiper CM, Voorn DA *et al.* Antiproliferative activity and mechanism of action of fatty acid derivatives of arabinofuranosylcytosine in leukemia and solid tumor cell lines. *Biochem. Pharmacol.* 67(3), 503–511 (2004).

48 Steingrimsdottir H, Gruber A, Palm C, Grimfors G, Kalin M, Eksborg S. Bioavailability of aciclovir after oral administration of aciclovir and its prodrug valaciclovir to patients with leukopenia after chemotherapy. *Antimicrob. Agents Chemother.* 44(1), 207–209 (2000).

49 Xia W, Hilgenbrink AR, Matteson EL, Lockwood MB, Cheng JX, Low PS. A functional folate receptor is induced during macrophage activation and can be used to target drugs to activated macrophages. *Blood* 113(2), 438–446 (2009).

• **Describes the fundamentals of folate-receptor targeting.**

50 Kumar S, Anselmo AC, Banerjee A, Zakrewsky M, Mitragotri S. Shape and size-dependent immune response to antigen-carrying nanoparticles. *J. Control. Release* 220(Pt A), 141–148 (2015).

51 Doshi N, Mitragotri S. Macrophages recognize size and shape of their targets. *PLoS One* 5(4), e10051 (2010).

52 Arainga M, Guo D, Wiederin J, Ciborowski P, Mcmillan J, Gendelman HE. Opposing regulation of endolysosomal pathways by long-acting nanoformulated antiretroviral therapy and HIV-1 in human macrophages. *Retrovirology* 12, 5 (2015).

53 Zhang G, Guo D, Dash PK *et al.* The mixed lineage kinase-3 inhibitor URMC-099 improves therapeutic outcomes for long-acting antiretroviral therapy. *Nanomedicine* 12(1), 109–122 (2016).

54 Ma JD, Lee KC, Kuo GM. HLA-B*5701 testing to predict abacavir hypersensitivity. *PLoS Curr.* 2, RRN1203 (2010).